Sex-dependent regulation of B cell tolerance by the miR-130b-ERα axis

Beatriz Herrero-Fernández[1], María del Pilar González-Molina[1], Laura Gámez-Reche[1], Ana M Prieto-Muñoz[1], Javier Sanz[1], Tania Gonzalo[1], Alba Moreno[1], MariPaz López-Molina[2], Laura Mañas[1], David Nemazee[3], Changchun Xiao[4], Laura Otero-Ortega[2], Alicia González-Martín[1,6]

[1] Department of Biochemistry, Universidad Autónoma de Madrid (UAM), Institute for Biomedical Research Sols-Morreale (IIBM), Universidad Autónoma de Madrid - Spanish National Research Council, Hospital La Paz Institute for Health Research (IdiPAZ), 28029, Madrid, Spain.

[2]Neurological Sciences Research Laboratory, Neurology and Cerebrovascular Disease Group, Neuroscience Area of Hospital La Paz Institute for Health Research, IdiPAZ (La Paz University Hospital - Universidad Autónoma de Madrid), Madrid, Spain.

[3] Department of Immunology and Microbiology, The Scripps Research Institute, La Jolla, CA, United States.

[4] Sanofi Institute for Biomedical Research, Suzhou, Jiangsu 215123, China.

[6] Corresponding author. Email: agonzalez@iib.uam.es

Abstract

Autoimmune diseases represent a timely health challenge due to their increasing incidence and lack of definitive cures. Autoreactive B cells play essential roles in several autoimmune diseases, including multiple sclerosis, lupus erythematosus and rheumatoid arthritis, which are more prevalent in women than men. However, the molecular mechanisms regulating these cells remain largely unknown. In this study, we identified miR-130b as a critical regulator of B cell tolerance through its suppression of Estrogen Receptor Alpha (ERα). Elevated levels of miR-130b impaired the elimination of autoreactive B cells by clonal deletion via downregulation of ESR1 (which encodes ERα) and PTEN, allowing their escape into peripheral tissues where they can contribute to autoimmunity. Deficiency in ERα expression alone was sufficient to allow the escape of self-reactive B cells to periphery in female, but not male, mice. Furthermore, elevated levels of miR-130b in patients with multiple sclerosis associated with increased disease activity and severity. Our findings reveal a previously unknown miR-130b-ERα axis that regulates B cell tolerance in a sex-specific manner and open new avenues to improve diagnosis and treatment of autoimmune diseases.

Main

Autoimmune diseases comprise more than 80 chronic, and often disabling, pathologies caused by dysregulated immune responses that target tissues, organs or cells of the

organism (referred to as self). Together, they affect 8-10% of the population (*1, 2*) and, for reasons that are poorly understood, their incidence is on the rise (*2, 3*). Notably, these pathologies are more prevalent in females than males (*4*). Most autoimmune diseases lack a cure, and existing treatments often entail significant adverse effects that reduce the quality of life of patients. In addition, the high costs of many of these therapies impose an economic burden on society.

Autoimmune diseases are characterized by a breakdown of immune tolerance, the series of mechanisms that ensure that our lymphocyte repertoire can eliminate a broad variety of invading pathogens and arising tumors without attacking self-tissues and organs. Autoreactive B cells play critical roles in autoimmunity through multiple mechanisms including generation of autoantibodies, presentation of autoantigens to T cells and secretion of proinflammatory cytokines (*5*). Previous studies showed that B cell tolerance is defective in patients with autoimmune diseases including multiple sclerosis, lupus erythematosus and rheumatoid arthritis (*6-8*). However, the molecular mechanisms that control B cell tolerance remain understudied.

B cell tolerance initiates in the bone marrow when a hematopoietic stem cell commits to becoming a common lymphoid precursor, which then develops into a proB and preB cell, the earliest stages of B cell development. During these stages, genetic rearrangements, known as V(D)J recombination, occur to form the immunoglobulin (Ig) heavy and light chains, respectively, resulting in an IgM molecule with a given specificity. Upon expression of IgM on the cell surface, the B cell enters the immature stage. The random and stochastic nature of V(D)J recombination ensures diversification of the antibody repertoire so that B cells can recognize a large diversity of foreign antigens (such as those from pathogens or tumor neoantigens), but also generates autoreactive B cell specificities. To prevent the exit of potentially harmful autoreactive B cells to the periphery, immature B cells are subjected to the central tolerance checkpoint. During this process, non-autoreactive cells exit the bone marrow to mature in the periphery, whereas autoreactive cells undergo Ig light chain rearrangement to acquire a new antigen specificity through the process known as receptor editing. If receptor editing eliminates autoreactivity, the cell proceeds to peripheral maturation and, otherwise, it can undergo additional rounds of receptor editing. If this mechanism fails to eliminate self-reactivity, the cells are removed from the repertoire by clonal deletion (apoptosis) (*9*). Additional tolerance checkpoints exist in the periphery, referred to as peripheral B cell tolerance, to regulate autoreactive B cells that have escaped central tolerance, including anergy, a state of non-responsiveness (*10*).

The IgM^b-macroself mouse model provides a potent *in vivo* platform for identifying novel regulators of B cell tolerance (*11*). These mice ubiquitously express an engineered superantigen that recognizes the constant region of the IgM heavy chain. In this model, early B cell development occurs normally and, upon IgM expression by immature B cells, binding of the superantigen occurs, mimicking self-recognition. This results in the elimination of all immature B cells through clonal deletion and, consequently, the absence

of mature B cells in peripheral sites, namely spleen and lymph nodes. Using this model, we previously stablished microRNAs (miRNAs) as main players in B cell tolerance, specifically miR-148a and miR-19b (*12, 13*). However, the identified mechanisms did not explain the increased susceptibility of women to autoimmune diseases compared to men. In this study, we identified miR-130b as a novel potent regulator of B cell tolerance. Mechanistic studies of the target genes of miR-130b uncovered Estrogen receptor 1 (*Esr1*) as essential for maintaining adequate control of central B cell tolerance in female mice only, revealing a previously unknown function for this protein that may contribute to the higher prevalence of autoimmune diseases in women. Finally, we demonstrate that increased levels of miR-130b in patients with autoimmunity associate with increased disease activity and severity.

Identification of common sequence motifs in lymphocyte-expressed miRNAs

MiRNAs, endogenous non-coding RNAs of approximately 22 nucleotides (nt), regulate cell function by imperfect binding to the 3´ untranslated region (UTR) of the messenger RNA (mRNA) of protein-coding target genes, resulting in a decrease in their protein levels through translational repression or mRNA degradation (*14*). Binding of miRNAs to their target mRNAs occurs mostly through their seed sequences, which locate within nucleotides 2-8. MiRNAs are grouped into miRNA families, with members of the same family sharing the same seed sequence. Previous studies showed that miRNAs regulate many processes of immune cell development and function (*15*), and that the expression of many miRNAs is dysregulated in patients with autoimmune diseases (*16*). This suggests fundamental roles for miRNAs in maintaining immune tolerance.

To uncover functionally relevant miRNA networks in B cells, we sought to identify common enriched motifs among miRNAs expressed in lymphocytes, reasoning that sequence patterns that occur in a group of related sequences often correlate with a biological function (*17*). For that, we performed a bioinformatic Multiple Em for Motif Elicitation (MEME) analysis of 101 lymphocyte-expressed miRNAs (Extended Data Table 1) (*18*). Since the nucleotides that comprise their seed sequences are the most relevant nucleotides for their function, and that the minimum sequence length allowed as input in MEME Suite was eight nucleotides, we introduced positions 1-8 of these miRNA families in MEME. The results from this analysis revealed multiple 4-6 nucleotide motifs that were common to different miRNAs (Fig. 1a). The nucleotide sequence of the motif that ranked third, GUGC, was highly conserved, suggesting functional significance. Eight miRNA families, miR-455, miR-33, miR-210, miR-19, miR-17, miR-148, miR-147 and miR-130 contained this motif (Fig. 1b). We then examined the expression levels of these families in B cells during development and upon activation. Most of them were expressed at moderate to high levels and, within families, the member with the highest expression levels was chosen for further analysis (Extended Data Fig.1a). This resulted in six individual miRNAs: miR-33a-5p, miR-210-3p, miR-19b-3p, miR-17-5p, miR-148a-3p and miR-130b-3p (referred to as miR-33a, miR-210, miR-19b, miR-17, miR-148a and miR-

130b from now on) (Fig. 1c). MiR-147 and miR-455 were undetectable or expressed marginally (if at all), respectively, in immature B cells and were consequently excluded from the study (Extended Data Fig.1b).

Interestingly, the resulting list contained the only two miRNAs previously identified as regulators of B cell tolerance to date, miR-148a and miR-19b (*12, 13*). This suggested that additional miRNAs within this list might control this process. In addition, the expression levels of these miRNAs throughout B cell development and activation were tightly regulated. MiR-17 and miR-130b displayed a similar pattern to that of miR-148a and miR-19b. Specifically, these miRNAs were expressed in proB and preB cells, downregulated in immature B cells, further downregulated in mature B cells in the periphery, and induced upon activation (Fig. 1d). On the contrary, miR-33 and miR-210, which were also regulated throughout development and activation, followed different expression patterns. Of note, the potential role of miR-17, a family member of the miR-17-92 cluster, in B cell tolerance was already analyzed in a previous study by the group, which excluded a major role for this miRNA in the process (*13*).

miR-130b regulates B cell tolerance

To validate the potential role of the identified miRNAs in the regulation of B cell tolerance, a hematopoietic stem and precursor cell (HSPC) transduction and reconstitution approach was performed in the mouse model of clonal deletion IgM^{b}-macroself as previously described (*12*). Briefly, donor C57BL/6J mice were inoculated with 5-fluorouracil (5-FU) to stimulate stem cell proliferation. Four days later, their bone marrow (BM) cells were isolated, enriched for HSPCs, transduced with MSCV-based retroviral particles encoding miR-130b, miR-33, miR-210 or an empty construct (control), and used to reconstitute lethally irradiated IgM^{b}-macroself mice for 8 weeks (Fig. 2a). This system provides a clean readout, since the presence of B cells in the spleen of these mice after reconstitution indicates a breakdown of B cell tolerance mediated by the transduced miRNA.

Analysis of the spleens of IgM^{b}-macroself mice after reconstitution revealed that increased levels of miR-130b promote the escape of a significant percentage of B cells from clonal deletion and their exit from the bone marrow to the periphery, with approximately 12% of splenic B cells among total splenocytes (Fig. 2b-d). Conversely, miR-33a or miR-210 did not mediate any substantial effect in this process, as the percentages of splenic cells were close to those detected in the spleens of IgM^{b}-macroself mice reconstituted with control-transduced HSPCs, which had approximately 1% B cells among total splenocytes (*12, 13*). These results demonstrate a function for miR-130b in the regulation of B cell tolerance. In line with this, increased levels of miR-130b have been found in B cells from patients with multiple sclerosis compared with healthy individuals (*19*). Elevated serum levels of miR-130b have been also associated with renal damage in patients with lupus nephritis (*20*).

Enrichment of predicted target genes of miR-130b in Estrogen receptor signaling

To identify the target genes through which miR-130b regulates B cell tolerance, we took advantage of the observation that it shares a minimal sequence motif, GUGCA, with previously identified regulators, miR-148a and miR-19b. Based on this, we hypothesized that these three miRNAs regulate this process through key common signaling pathways. To select potential target genes, the predicted targets from these miRNAs were retrieved from miRDB. As shown in the Venn Diagram, this resulted in a list of 110 targets that were common to the three miRNAs (Fig. 3a and Extended Data Table 2). These targets were then subjected to Ingenuity Pathway Analysis (IPA) to identify signaling pathways highly enriched in proteins that may be playing a regulatory role in central B cell tolerance. Unexpectedly, Estrogen Receptor Signaling was retrieved as the top-ranked canonical pathway (Fig. 3b,c). Eight predicted targets containing binding sites for these miRNAs formed part of this pathway: *Cfl2*, *Esr1*, *Igf1*, *Med12L*, *Prkaa1*, *Pten*, *Runx2* and *Sos2*.

Since miRNA regulation is cell-dependent, we next determined which of these proteins are expressed in immature B cells. For this, immature B cells from bone marrow from C57BL/6J mice were stained with antibodies against cell markers CD19, CD93 and IgM coupled with fluorophores and purified through fluorescence-activated cell sorting (FACS). This was followed by extraction of total RNA from these samples and analysis of the expression levels of these targets using quantitative real-time polymerase chain reaction (qRT-PCR). *Cfl2*, *Esr1*, *Prkaa1*, *Pten* and *Sos2* exhibited moderate to high expression levels in immature B lymphocytes (Fig. 3d). In contrast, *Igf1*, *Med12L* and *Runx2* displayed marginal or negligible expression and were therefore excluded from further analyses.

Targeting of ERα and PTEN by miR-130b

As the targetomes of miRNAs are also cell context-dependent (*15*), we assessed whether these targets are regulated by miR-130b in the immature B cell line WEHI-231. This cell line recapitulates the clonal deletion process when its IgM molecule is bound with an anti-IgM antibody, mimicking self-recognition and resulting in a fraction of cells undergoing BCR-engagement-induced apoptosis (clonal deletion) as it occurs during central tolerance. Stable WEHI-231 cells expressing or not increased levels of this miRNA were generated through transduction with control- or miR-130b-expressing retroviruses that also encode the GFP protein, followed by enrichment by FACS. WEHI-miR-130b cells showed more robust miR-130b expression compared with WEHI-control cells, as validated through Taqman assays (Extended Data Fig. 2a).

To confirm that this *in vitro* model recapitulates the effect of miR-130b on central tolerance, stable WEHI-control and WEHI-miR-130b cells were stimulated with an anti-IgM antibody or left untreated, and analyzed for apoptosis 72 hours later. As expected, a fraction of control cells underwent apoptosis, while increased expression of miR-130b

reduced the percentage of apoptotic cells by approximately 10% (Fig.4a). The proliferation rate of these cells was also analyzed by Cell Trace Violet dilution. These experiments indicated that miR-130b does not affect cell proliferation (Fig. 4b).

We next stimulated both stable WEHI-231 cell lines with anti-IgM for 14 hours, a time in which cells are signaling for apoptosis (clonal deletion) but still have not initiated the death process. Cells were then harvested, and total RNA was purified to measure the expression levels of these target genes by qRT-PCR. Among the selected targets, *Esr1* (which encodes for Estrogen receptor alpha; ERα) and *Pten* (which encodes the tumor suppressor PTEN) were downregulated by 70% in cells with increased levels of miR-130b compared to control cells (Fig. 4c). The levels of the other genes were not downregulated by miR-130b. The protein levels of ERα and PTEN were also determined in these cell lines by Western blot. These results confirmed the miR-130b-mediated reduction of the expression levels of both ERα and PTEN (Fig. 4d).

In addition, reporter assays were performed to confirm whether miR-130b regulates *Esr1* and *Pten* through direct binding to their cognate binding sites in their 3´UTR regions (Extended Data Table 3). These assays showed that miR-130b decrease the expression levels of the reporter gene fused to the 3´UTR of both target genes (Fig. 4e). In addition, this effect was completely or significantly lost for *Esr1* and *Pten*, respectively, when the binding sites of the miRNA were mutated. Overall, our data show that the expression levels of both ERα and PTEN are reduced by miR-130b though its binding to their cognate binding sites in their 3´UTRs. While *Pten* is a known regulator of central B cell tolerance (*12, 13, 21*), the potential role of *Esr1* in this process had not been previously analyzed.

ERα functions as a gender-specific regulator of central B cell tolerance

To validate whether these targets regulate B cell tolerance, we obtained mice deficient in *Esr1* and *Pten* and used their bone marrow cells to reconstitute lethally irradiated IgM^{b}-macroself mice (Fig.5a). After 8 weeks, the spleens of these mice, as well as those of a group reconstituted with cells from control mice, were analyzed for the escape of B cells to the periphery.

The role of PTEN in B cell tolerance had been previously established by us and others (*12, 13, 22*). When bone marrow cells from donor mice with B cell-specific deletion of *Pten* (CD19Cre;*Pten*$^{fl/fl}$) were used to reconstitute irradiated IgM^{b}-macroself mice, a drastic percentage of B cells was observed in the spleens of those mice 8 weeks later compared with the control group reconstituted with bone marrow cells from C57BL/6J wild type mice, which had almost no B cells in the spleen (Fig.5b-d).

Since ERα is expressed and functions differentially in women and men, we specifically addressed the potential role of *Esr1* in females by reconstituting irradiated IgM^{b}-macroself mice with bone marrow cells from *Esr1*-deficient mice (*Esr1* KO). As expected,

mice in the control group had a nearly complete absence of B cells in their spleens. In contrast, deficiency of *Esr1* was sufficient to enable escape from B cell tolerance, as shown by the presence of approximately 14% of B cells in the spleens of IgM^{b}-macroself mice reconstituted with bone marrow cells from *Esr1*$^{-/-}$ mice (Fig. 5e-g). These results demonstrate that ERα is required for the adequate establishment of central B cell tolerance, a previously unknown function for this receptor. Next, we asked whether this effect was sex-specific. To address this, the same experimental approach was performed using both female and male mice. Interestingly, the requirement for ERα in B cell tolerance was observed in female, but not male, mice (Fig. 5h-j), uncovering a novel gender-dependent miR-130b-ERα mechanism promoting autoimmunity.

Increased serum levels of miR-130b in patients with autoimmunity associate with worse disease activity and severity

Previous studies have shown that circulating B cells from patients with multiple sclerosis express higher levels of miR-130b than those of healthy individuals (*19*). Since B cells are a major source of serum extracellular vesicles (EVs) (*23, 24*), we next explored whether the levels of miR-130b in EVs might be used as a biomarker for patients with autoimmunity. EVs offer several advantages for biomarker discovery, as they can be readily isolated from serum, providing a minimally invasive approach compared to direct analysis of B cells. Additionally, EVs protect miRNAs from degradation, ensuring a more stable and reproducible detection of miR-130b levels in circulation.

To assess this, serum samples were collected from a cohort of patients with multiple sclerosis (Extended Data Table 4), followed by EV isolation and quantification of miR-130b by NGS. Our analysis revealed that higher levels of miR-130b were associated with more severe disease activity, as indicated by an increase in new central nervous system lesions (Fig. 6a). This was accompanied by accelerated cognitive decline and brain atrophy, as evidenced by reduced volumes of gray matter, cortical gray matter, total brain, caudate nucleus and total cerebellum (Fig. 6b-g). Thus, the levels of miR-130b in serum EVs correlate with increased disease severity in patients with multiple sclerosis and, therefore, could serve as a potential biomarker.

Discussion

In this study, we identified miR-130b as an essential regulator of B cell tolerance. Increased levels of miR-130b compromised clonal deletion resulting in the escape of self-reactive B cells to the periphery. Once in the periphery, these cells can recognize self-antigens and, hence, contribute to the onset and progression of autoimmune diseases. The expression of miR-130b in proB and preB cells was relatively high, downregulated in immature B cells, further downregulated in mature B cells in periphery, and induced upon activation, suggesting that its levels need to be low during central tolerance as part

of an integrated molecular circuitry that controls this process. In line with this, a previous clinical study correlated upregulation of miR-130b levels with renal damage in patients with early lupus nephritis (*20*).

An intriguing question in immunology arises from the observation that the incidence of many autoimmune diseases is higher in women than men (*4*). A recent population-based cohort study of 22 million individuals in the UK investigated the incidence and prevalence of 19 of the most common autoimmune diseases between 2000 and 2019. Together, these autoimmune disorders affected 10.2% of the population over the study period with the percentage rising to 13.1% in women and decreasing to 7.4% in men (*2*). Despite considerable research efforts to elucidate the gender disparity in autoimmune development, the underlying molecular mechanisms remain incompletely understood. In this study, we identified Estrogen receptor signaling as a key signaling pathway that control this process. Further examination of the target genes included in this pathway revealed that ERα, a hormone receptor with markedly different expression levels and functions in females than in males (*25*), and PTEN play important roles as regulators of central B cell tolerance.

ERα regulates the development and physiology of the reproductive system, including during pregnancy, and also plays relevant roles in other cell types, including immune system cells (*26*). ERα is expressed in B cells and has been previously shown to prevent autoimmunity. *Esr1* germline knockout mice (*Esr1*$^{-/-}$) developed autoimmune glomerulonephritis with spontaneous formation of splenic germinal centers, proteinuria, infiltration of B cells in the kidneys, damage of tubular cells and presence of serum anti-dsDNA antibodies at one year of age (*27*). Another study partially attributed this autoimmune phenotype to an ERα-mediated control of follicular helper T cell responses (*28*). We now provide genetic evidence demonstrating that ERα is required to control autoreactive B cells from exiting the bone marrow to periphery where they could damage self-tissues in female, but not male, mice. Deletion of *Esr1* allowed escape of autoreactive B cells from the central tolerance checkpoint, which probably contributed to the autoimmune disease that developed in *Esr1*$^{-/-}$ mice. In humans, a previous clinical study determined the expression levels of ERα in freshly isolated T lymphocytes from patients with systemic lupus erythematosus and healthy individuals and found significantly lower levels of this protein in the patients with lupus compared with the control group (*29*). Concurrently, published studies showed that decreased estrogen levels in women at menopause correlate with increased susceptibility to autoimmune diseases (*26*).

PTEN, the other identified target within the Estrogen receptor pathway, had been previously shown to regulate B cell tolerance and prevent autoimmunity. *Pten*$^{+/-}$ mice developed lethal autoimmunity (*21*) and *Pten* deficiency broke central B cell tolerance and impaired B cell anergy (*12, 22*). The targeting of different proteins within the same signaling pathway by miRNAs, specifically *Esr1* and *Pten,* suggests functional

cooperation between these targets to tightly regulate the apoptotic machinery required for the removal of autoreactive B cells.

Previous studies on the reproductive system showed that the levels of PTEN fluctuate during the normal menstrual cycle, suggesting its regulation by hormones in the endometrium. 17β-estradiol (E2) stimulates both genomic and nongenomic ERα actions in this system, and the protein levels of PTEN are the highest in uterine epithelial cells during the E2-driven phase of the menstrual cycle (*30*). Another study showed that E2 signaling increases the levels of PTEN and that cytosolic ERα forms a complex with PTEN in an E2-dependent manner, consistent with functional cooperation between these targets (*31*). If similar mechanisms were in place in immature B cells, the simultaneous regulation of the expression of ERα and PTEN by miR-130b could result in a gender-biased regulation of B cell tolerance.

Since miRNAs are frequently contained within circulating extracellular vesicles in humans (*32*) and the levels of miR-130b are elevated in B cells from patients with multiple sclerosis (*19*), we investigated whether miR-130b in EVs could serve as a biomarker for autoimmune diseases. EVs protect miRNAs from degradation, enabling stable detection of molecular signals in circulation and offering a readily accessible, cost-effective alternative to direct cell-based analyses for clinical applications. Notably, increased miR-130b levels in EVs from patients with multiple sclerosis correlated with more severe disease progression, characterized by the formation of new brain lesions, and accelerated cognitive decline and neurodegeneration. These findings suggest that elevated miR-130b levels in EVs may reflect increased autoreactive activity and potentially serve as a biomarker of disease severity in multiple sclerosis.

Overall, our study identified a sex-dependent miR-130b-ERα axis as a critical regulator of B cell tolerance and autoimmunity. These findings advance our current understanding of B cell tolerance and provide new insights into the molecular mechanisms underlying gender differences in autoimmune diseases, with potential diagnostic and therapeutic implications for patients with these diseases.

Figures

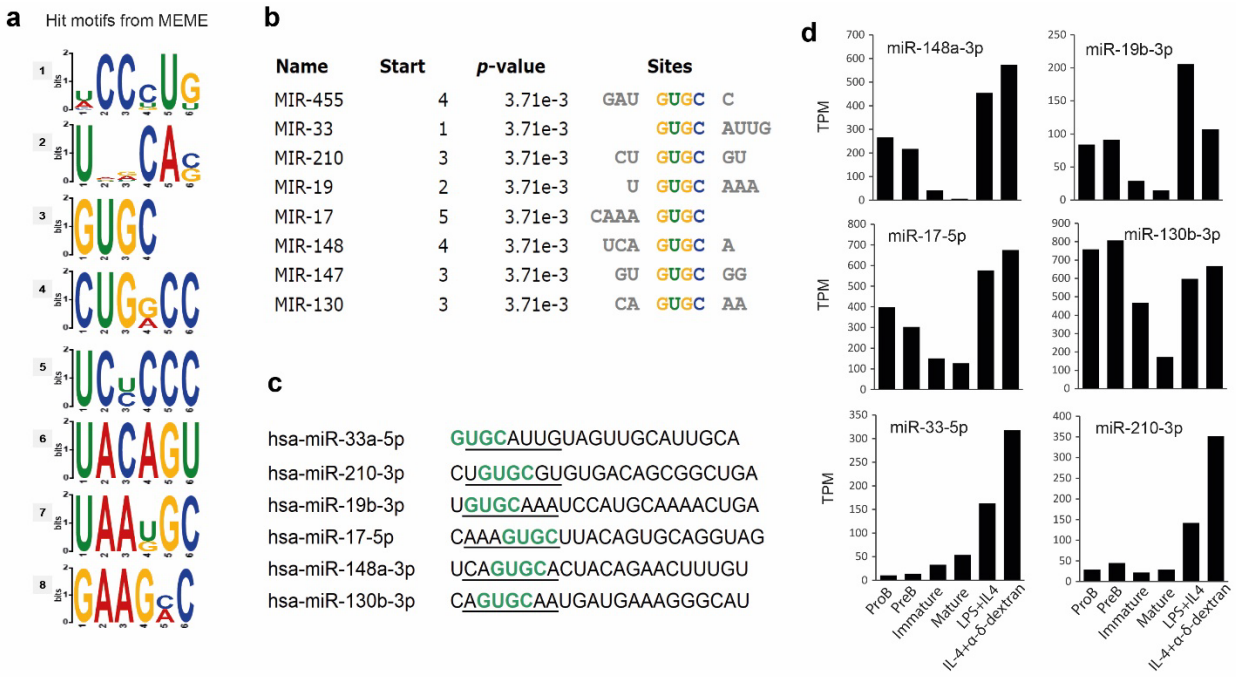

Fig. 1| Motif analysis of lymphocyte-expressed miRNAs. a, Hit motifs from Multiple Em for Motif Elicitation (MEME) analysis of 101 lymphocyte-expressed miRNA families. Nucleotides 1-8 of each miRNA, that contain their seed sequence, were used as input for the analysis. **b,** MiRNA families containing the conserved GUGC motif, ranked third by MEME. **c,** Representative miRNA members within each family with the highest expression levels in B lymphocytes. The seed regions are underlined, and the GUGC motif highlighted in green. **d,** Expression levels of miRNAs in **c** throughout murine B cell development and activation as indicated. The graphs in **d** were generated based on previously published data (*18*).

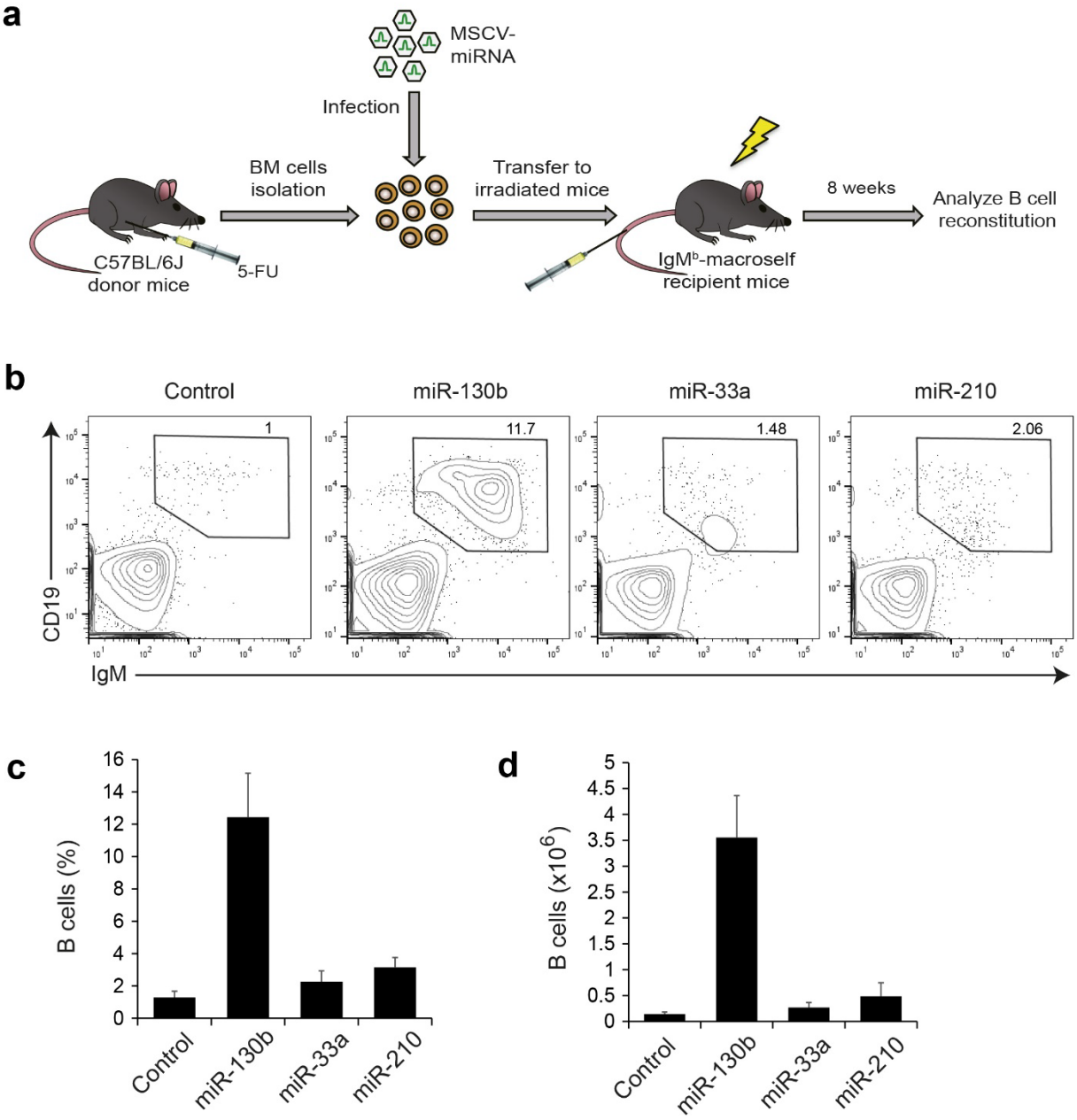

Fig.2| MiR-130b promotes escape of B cells from central B cell tolerance. a, Schematic representation of bone marrow transduction and reconstitution experiments in the murine B cell tolerance model IgM^b-macroself. **b,** Representative flow cytometry contour plots showing splenic B cells of IgM^b-macroself mice reconstituted with bone marrow transduced with miR-130b, miR-33, miR-210 or control vector, as indicated. Numbers above the outlined area indicate percent of CD19$^+$-IgM$^+$ cells (splenic B cells) among total splenocytes. **c,d,** Bar graph showing the percentages (**c**) and total numbers (**d**) of splenic B cells of all mice analyzed in **b**. Graphs represent mean + s.e.m. Data are pooled from five independent experiments in **c**,**d**. n=5 mice/group.

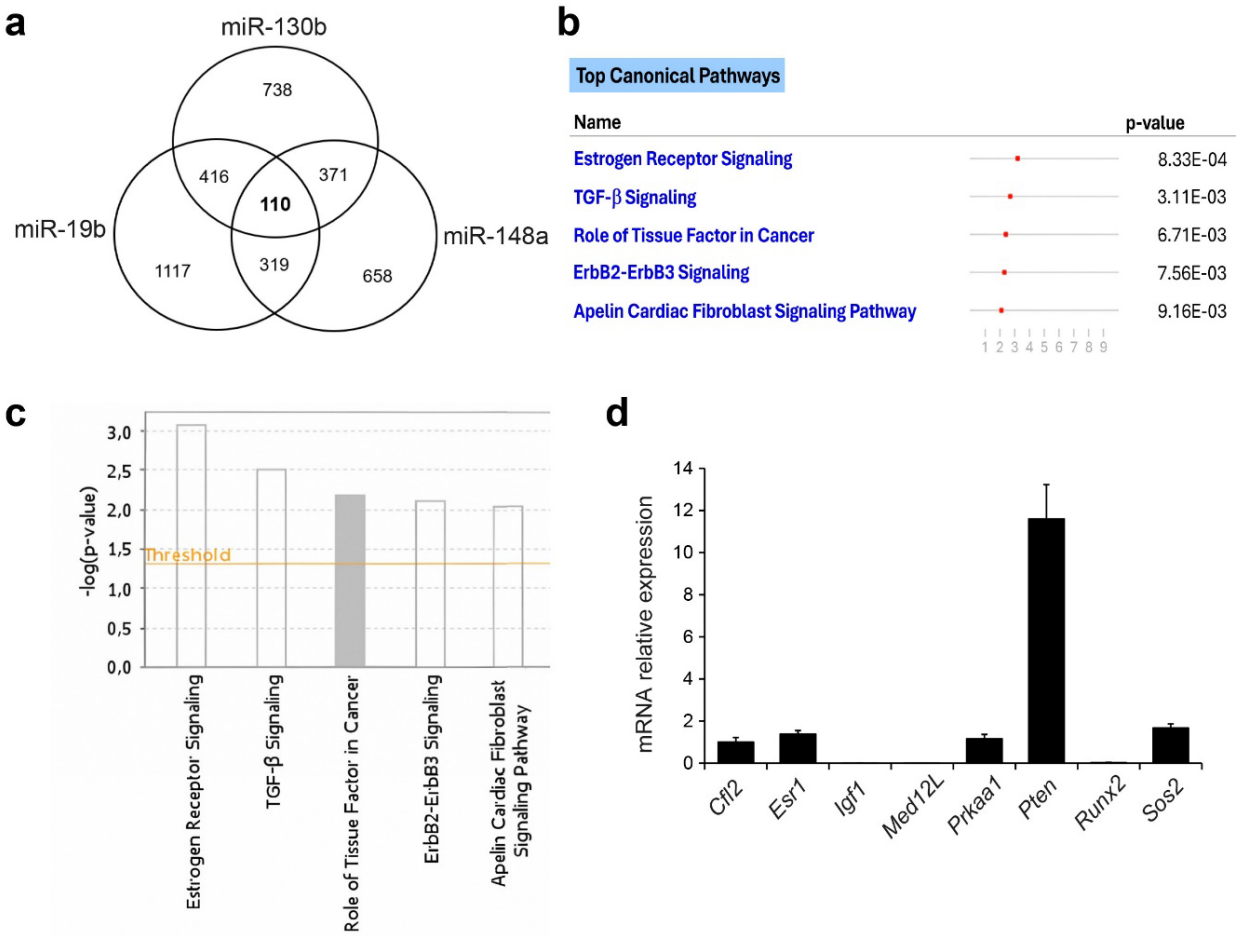

Fig.3| The Estrogen receptor signaling pathway is enriched in targets regulated by miRNAs that control B cell tolerance. a, Venn diagram of the predicted target genes (miRDB) of miR-130b, miR-19b and miR-148a, the miRNAs identified as regulators of B cell tolerance to date. **b,c,** Top canonical pathways identified through Ingenuity Pathway Analysis (IPA) of the 110 common target genes of these miRNAs. The orange line in **c** represents the threshold for a positive z-score. **d,** Bar graph showing the relative expression of all the target genes included in the Estrogen receptor signaling pathway, as indicated, in primary murine immature B cells sorted from C57BL/6J mice and analyzed by qRT-PCR. Graphs show mean + s.d. Immature B cells sorted from bone marrow of 19 mice were pooled in **d**, and technical triplicates are shown.

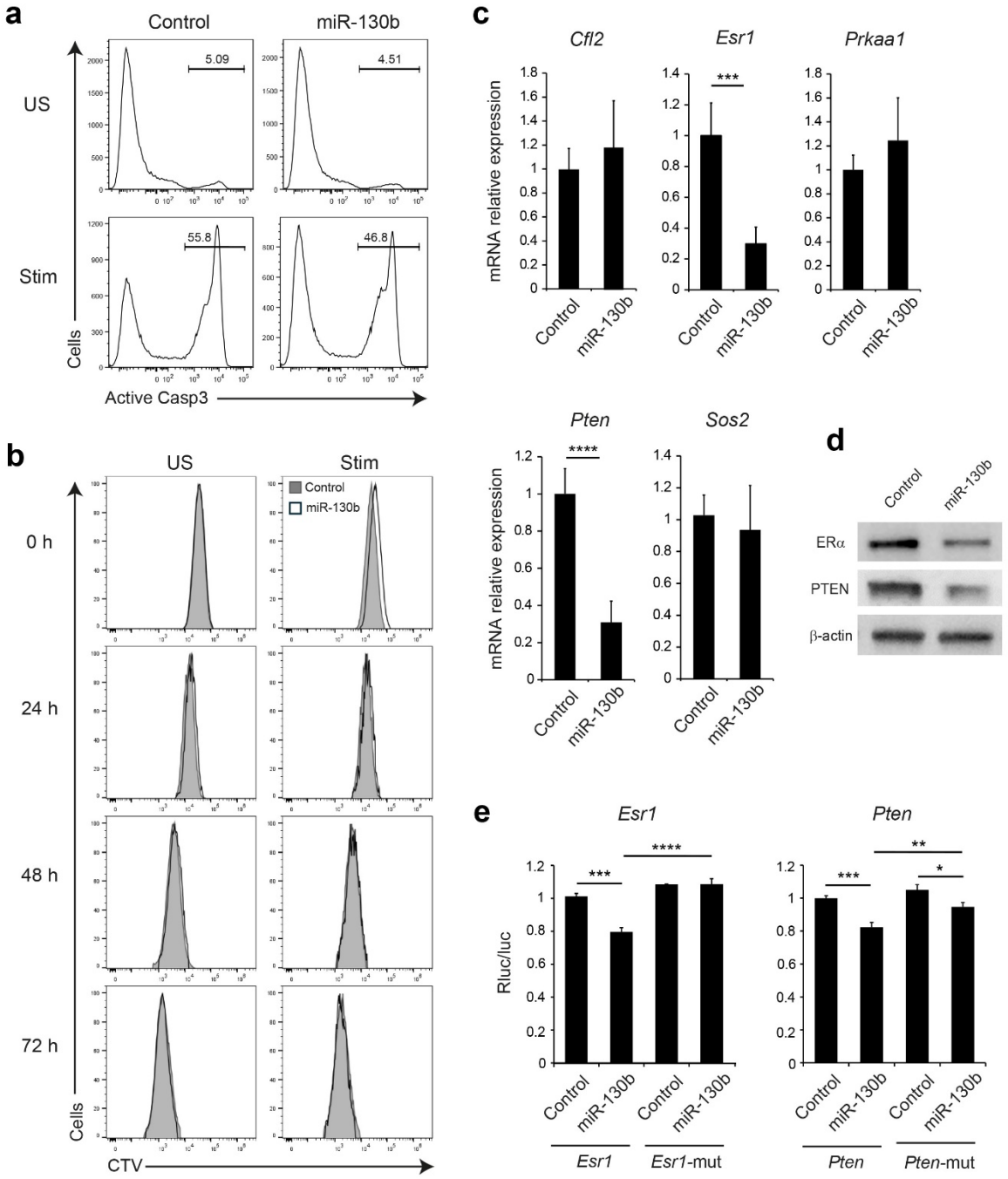

Fig. 4| MiR-130b targets *Esr1* and *Pten*. a, Representative histograms showing active caspase 3 analysis of WEHI-control and WEHI-miR-130b cells left unstimulated (US) or stimulated (Stim) with anti-IgM (2μg/ml) for 72 hours. **b,** Overlay histograms of cells as of **a** stained with Cell Trace Violet (CTV) and analyzed at different time points, as indicated. **c,** Bar graphs showing relative expression of *Cfl2*, *Esr1*, *Prkaa1*, *Pten* and *Sos2* of WEHI-control and WEHI-miR-130b cells stimulated for 14 hours. **d,** Immunoblot analysis of protein levels of ERα and PTEN, as well as β-actin (loading control), in these cells. **e,** Bar graphs showing normalized expression of renilla luciferase reporter protein fused to the wild-type 3′ UTR of *Esr1* or *Pten* and 3′ UTR of *Esr1* or *Pten* with mutated binding sites for miR-130b, cotransfected with an expression vector encoding miR-130b or an empty vector (control). The levels of the reporter protein were analyzed 24 hours post-transfection and normalized to that of a constitutively expressed firefly luciferase. Graphs show mean + s.d. Data are representative of two independent experiments in **a**, **b**, **d** and **e**, and pooled from two independent experiments in **c**. Statistical significance was determined with an unpaired two-tailed Student's t test. * $P \leq 0.05$, ** $P \leq 0.01$, *** $P \leq 0.001$ and **** $P \leq 0.0001$.

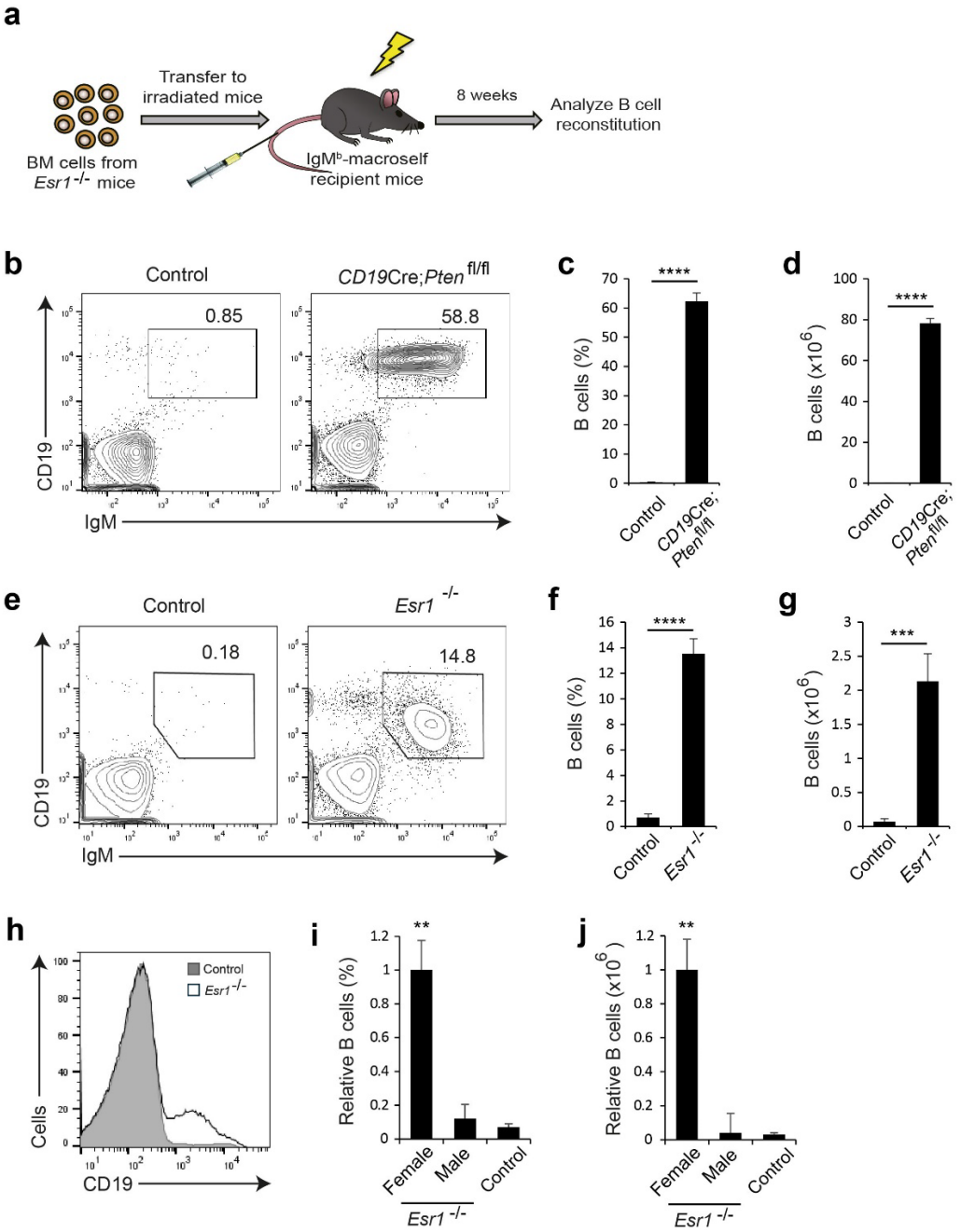

Fig. 5| ERα deficiency impair B cell tolerance in a sex-dependent manner. a, Outline showing bone marrow reconstitution experiments of IgM^b-macroself mice. **b,e,** Representative contour plots showing splenic CD19$^+$-IgM$^+$ B cells in recipient IgM^b-macroself mice reconstituted with bone marrow (BM) cells from donor *Esr1$^{-/-}$, CD19*Cre*;Pten*$^{fl/fl}$ or control mice, as indicated, analyzed by flow cytometry 8 weeks after reconstitution. Mice reconstituted with *Esr1$^{-/-}$* BM cells were all female. **c,d,f,g,** Bar graphs showing the percentages (**c,f**) and total numbers (**d,g**) of splenic B cells of all mice analyzed in **b** and **e**. **h,** Representative overlay histogram showing percentages of CD19$^+$ B cells in female and male IgM^b-macroself mice reconstituted with BM cells from *Esr1$^{-/-}$* KO mice. **i,j,** Bar graphs showing relative CD19$^+$-IgM$^+$ B cells percentages (**i**) and numbers (**j**) in all mice analyzed in **h**, and pooled male and female IgM^b-macroself mice reconstituted with BM cells from control mice. Female values were arbitrarily set to 1 and all other conditions shown relative to this group. Graphs represent mean + s.e.m. Data are representative of two independent experiments. n=7 mice (control group), n=5 (*CD19*Cre;*Pten*$^{fl/fl}$ and male *Esr1$^{-/-}$* groups) and n=9 mice (female *Esr1$^{-/-}$* group). Statistical significance was determined with an unpaired two-tailed Student's T test. ** P ≤ 0.01, *** P ≤ 0.001 and **** P ≤ 0.0001.

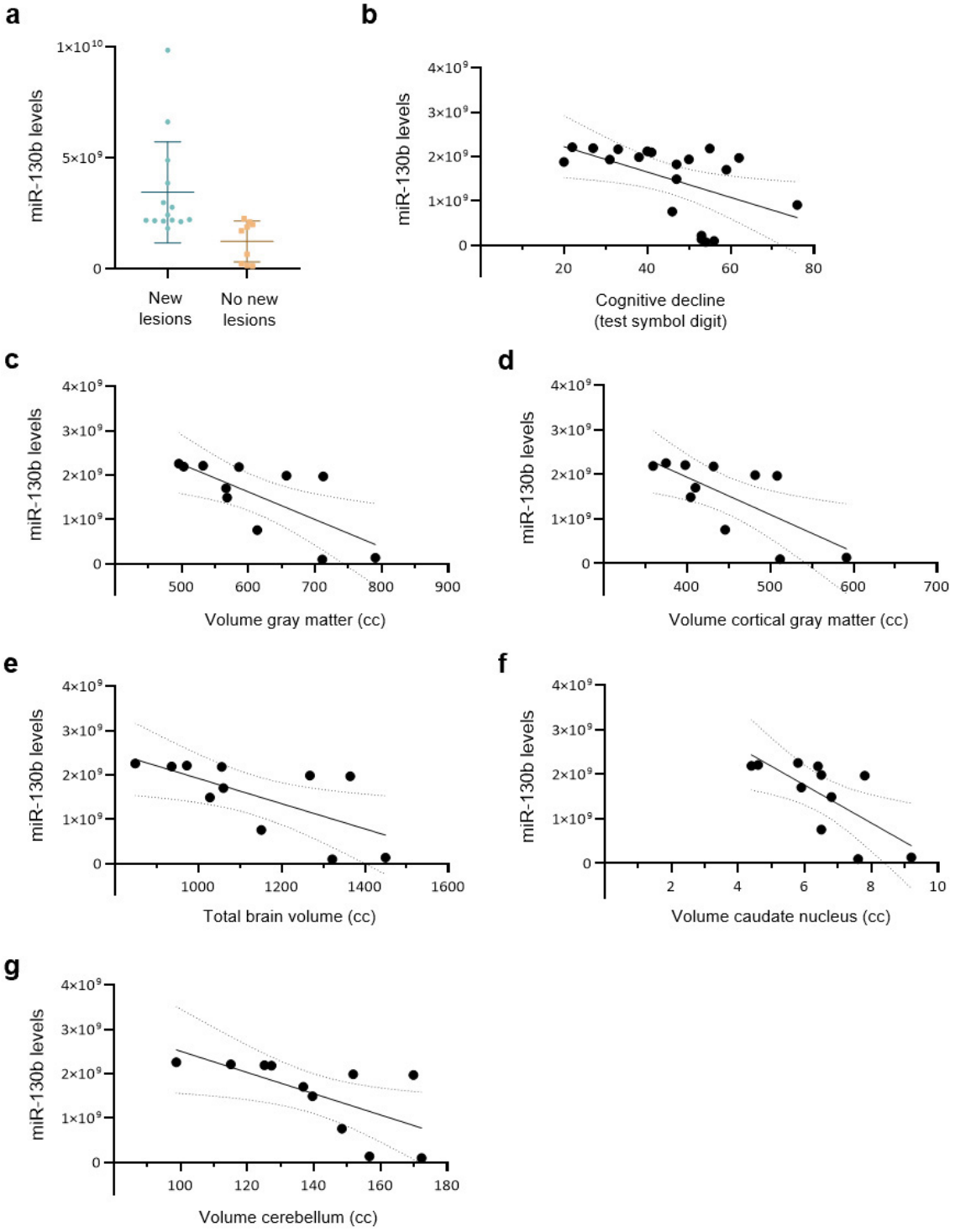

Fig. 6| Elevated miR-130b in circulating extracellular vesicles associated with new central nervous system lesions, and greater cognitive decline and atrophy in patients with multiple sclerosis. a, Levels of miR-130b in circulating extracellular vesicles (EVs) of patients with multiple sclerosis developing or not new central nervous system lesions, as determined by magnetic resonance imaging. **b-g,** Cognitive decline (**b**) and volume of gray matter (**c**), cortical gray matter (**d**), total brain (**e**), caudate nucleus (**f**) and total cerebellum (**g**), as a function of miR-130b expression. Statistical significance was determined with a Mann-Whitney U test (n= 41 patients). *** P ≤ 0.001.

Extended data

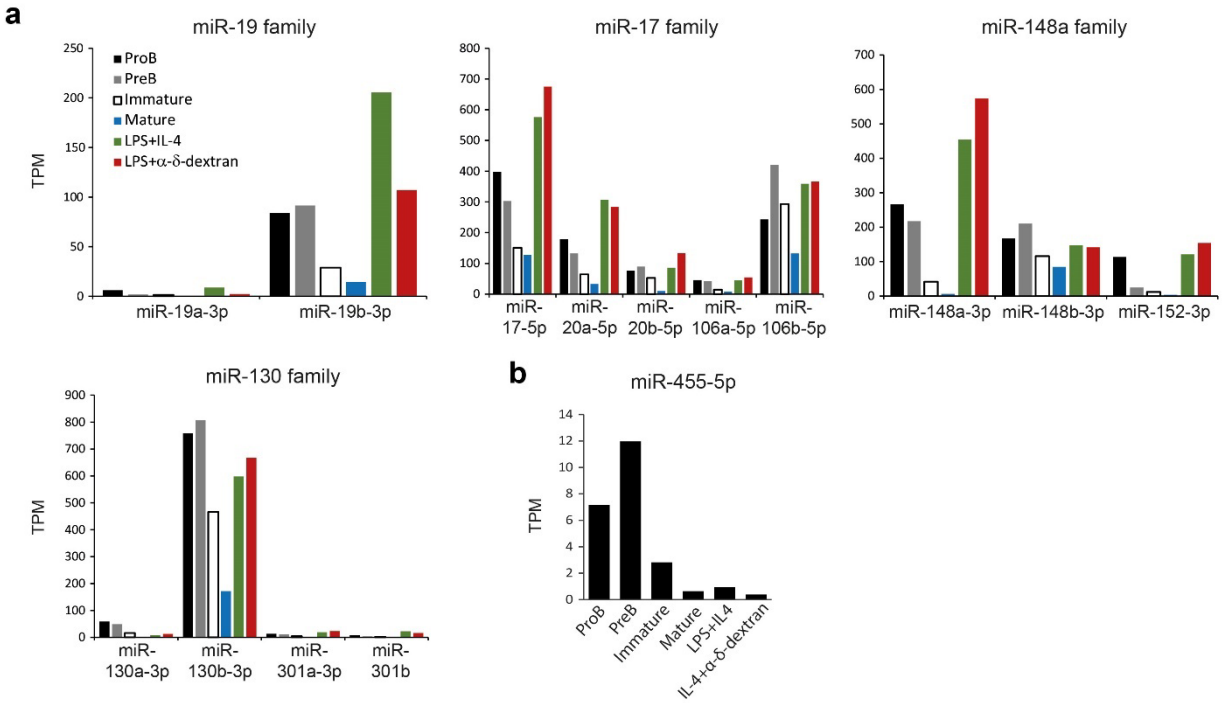

Extended Data Fig. 1| Expression levels of miRNA families identified by MEME analysis and miR-455-5p. a, b, Bar graph showing expression levels of individual miRNAs within the miRNA families identified by MEME analysis (**a**) and miR-455-5p (**b**) at different stages of B cell development and activation, as indicated. The graph was generated based on previously published data (*18*).

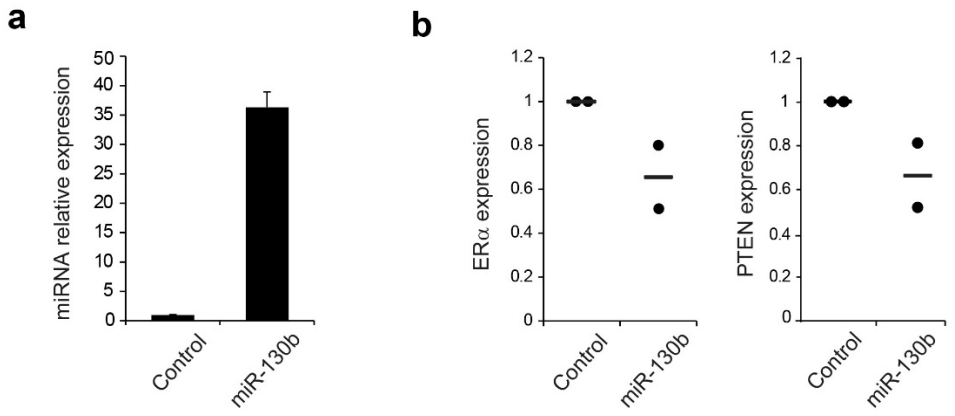

Extended Data Fig. 2| Regulation of ERα and PTEN by miR-130b. a, Bar graph showing relative expression of miR-130b in WEHI-control and WEHI-miR-130b cells determined by Taqman Assay. **b,** Graphs showing quantification of protein expression levels of ERα and PTEN in WEHI-control and WEHI-miR-130b cells determined by immunoblot in two independent experiments. The levels of these proteins were normalized to that of β-actin (loading control).

Extended Data Table 1| List of lymphocyte-expressed miRNAs used for Multiple Em for Motif Elicitation (MEME) analysis.

Lymphocyte-expressed miRNA families		
Let-7	miR-194	miR-342
miR-1	miR-1948	miR-345
miR-10	miR-196	miR-350
miR-101	miR-1964	miR-351
miR-103	miR-1981	miR-361
miR-1198	miR-199	miR-362
miR-122	miR-203	miR-374
miR-127	miR-204	miR-375
miR-128	miR-21	miR-378
miR-130	miR-210	miR-423
miR-132	miR-219	miR-425
miR-138	miR-22	miR-450
miR-139	miR-221	miR-451
miR-140	miR-223	miR-455
miR-142	miR-23	miR-504
miR-143	miR-24	miR-505
miR-146	miR-26	miR-511
miR-147	miR-27	miR-542
miR-148	miR-28	miR-574
miR-15	miR-29	miR-598
miR-150	miR-296	miR-652
miR-155	miR-298	miR-671
miR-17	miR-30	miR-672
miR-181	miR-31	miR-674
miR-184	miR-32	miR-676
miR-185	miR-324	miR-7
miR-186	miR-326	miR-700
miR-188	miR-328	miR-744
miR-19	miR-33	miR-8
miR-190	miR-330	miR-872
miR-191	miR-331	miR-92
miR-192	miR-339	miR-95
miR-193	miR-34	miR-96
miR-1934	miR-340	

Extended Data Table 2| Predicted common target genes of miR-130b, miR-19b and miR-148a identified through RDB target mining.

Gene name		
AGO1	FAM43A	PTGES3
ABCA1	FBXO28	QKI
ABCB7	FMR1	RAB14
AGFG1	GPCPD1	RNF38
AKAP1	GTF2H1	ROBO2
ANGEL2	HECW2	RPS6KA5
ARFIP1	IGF1	RUNX2
ARHGAP21	IL15	SBF2
ATG14	ING2	SECISBP2L
ATXN1	INHBB	SERPINE1
B4GALT5	INO80	SGMS2
BLCAP	ITGB8	SIX4
BMP3	JARID2	SKIDA1
BTAF1	KIAA1217	SLC12A7
C5orf30	LDLR	SNX27
CAMSAP2	LRP2	SOS2
CBLB	MAP1B	ST8SIA3
CCDC6	MDFIC	SULF1
CDK19	MDM4	SYT6
CDS1	MED12L	TBC1D8
CEP55	MIER1	TENT2
CFL2	MLLT6	TGFBRAP1
CHST1	MTCL1	TMEM63B
CLCN6	MTMR10	TMEM9B
CNOT6	NECTIN3	TNRC6C
DCP2	NME7	TSPOAP1
DDX6	NOL4	UBE2D3
DENND4C	NPEPL1	USP33
DICER1	NPTN	USP6
EMX2	PHF20	VPS37A
EOGT	PIGS	WDR20
EPS15	PITPNM2	ZBTB18
ERBB3	PLAA	ZBTB20
ESR1	POU3F2	ZDHHC23
F3	PPP6R1	ZFYVE26
FAM104A	PRKAA1	ZNF217
FAM234A	PTEN	

Extended data Table 3| *Esr1* and *Pten* 3′ UTR cloned fragments for reporter assays, and mutated binding sites for miR-130b (*Esr1* and *Pten*).

***1. Esr1* 3'UTR**

GAGCTCCCAGGCTCCCCGAAAGGTTCTGAGAATCCCTGCAACATTTTACCCATGTCATGTATGACTAGCAGAATTCTG
TCTCCTGCGTACACTGTGGCATGCATCCACCACCAGTGGCTTTCTAGTATGAGTGGCCATTTATTTGCTTGCTCAGTTC
TTAGTGGCATGTCTTCTGTTGGGAACAGGCAAAAGGGATTCCAGGGCTAAATCTTGGTAACAGCTCTCTTTCTCCCT
TTGCTACGTCACTAACTATGAGGATTCCTATAGTCTTCAGTCTTCATGAATGAATTGAGATAACTGCATTGAAGCTACT
TGTTGAGACCCAAGCCTAGAGAGTAAACATTTCACCTCTGATAAGCACTTCATAATGGCTCCAAGAGGAAGCCTCAG
CAAAGACTTCAAAGTGGCTCCTTTAATTGAAGTCGTTGACAAAGCGATCTCATGGCTTCCTAATAGCACCCGCTTGC
ATTCCTATAGCAACATGTGACTTTATTAAAGGGAAATCTTGAGCCCCTATAGGAATATGTGATGCACACAGAAAAGGA
AGATGCCCCCAGTTGTCAAGACCATGTCAACTCAATACAGTCAACCTTTTCACTTCTTAAAGTGTCAGCTGCCGAGTA
TTATATACATGGTGGGTTCTAGACAATTCTTGCTTCCCATGACTTGTGGGAAACAGAAAGTCTATTTCAGTTAATACCC
TGGAATGAATTAGTCTCCTTCATGAGGGCTGTAGGGTGTGTTGATTTTAATTTGATTTCATTTTATAATAGTCTTCTGCC
CCTGGGGCTTGCAGTAAAGGCAGCTTGAGGACCTGTTCTGGTAAACTGGACATTCTTCAGCACAGGATGCTAGCCT
TGTCTCTTCCCTGATGTCAATTGCCCTAAATTGTTACCATGTAGATTGATCAAGGGCAGTCACAATGAACCTGCAAGC
TGGTGACAATTTTTTGGTTTGTTTAGTTTTATTCTTGGGGGCAGGGAACAAGTAATGTATGGGCAATGACTGTGACT
CGGAGGAGTCTAAGAAGGAAAGTAAGGGAGAAATGTGGAGAATGACCTGGCCAGGGCAGCAGCTTCCCAGAGGT
GCACCTCACAGATCCCACCATGCACAGTGAGGCTGCTCTGGGATCCATGGGCTGACTTCACTTACATTTCAGGTATG
AGCCTGATTGGAAGAGGTGACATCAGATACCTGTGTTCCTGTAGATGCTCCAGGAACTTGGGGAAAGGCATGGGG
GCAAGATCTTGGAGCACTCATGACTCAAGCTGTTGAGAAGTTGCTCAGACTAGACTGTGCTTGATTATTCTGAACTC
ATCCAAAAACCAGCTAGTGAGATCTTGGGGAGAAAAATTTCTTCCTCAACACAGTTCATGATCTTAAATTTTGTAAAC
TAGAAATGATGAATGACCAGAATTGGGTCATGAGAGTCCTTTGAACAAGGGGATAAAAAGGAAGACTTACTCTATC
CACAGCCACCCAAGACCTCTGGGGTCTTGGTCTCTCTAGTACAACTAAGGATTACTTCCTTTTCCAAACCAAAATGAA
AGTTCAGTTTCCATCCCGGACTTCATGATCTATAATTTGAACTCCATTGAGATATGATGGGTTAGCCAAAACCTAGGTG
AATGGCTAGGCTTCTCTTGGCCTGTACTTTTTGGAATGGTGGGTTCCATTAATTTCTGCTCTCCCAGTTAACTGACTAT
CAAAGATGTGGAAACTGGGAGAGCCAATTTTTCTTCTTATTTTTTTTAAATTTCTCATACTTGTTCATCAAATTCAAGG
ACAATTTTATGTATATGCTTTAAGAACATGTTTAAGAACCTAACTCTTTTGTTTGTGTTTAAGAAGCACCTTATATAGTA
TAATATATATTTTTGTTGAAGTTTAATTGCTTGTTTATTGGACAATTGAATGTAATAGTTATGTTCTGAGTTTTAATTTGA
TTGGGTTTAACACTGCAAAAGCCAAGGGGAAAATATTTAGTTTGTTTTTTTTTTTTTTTTTTGTAGACGTTTCAAACT
ACCGTGTCATGTATGCAGTTATTAATGCCTAAAGCCTTGTGATTTTCATTTAAATGAAGATCACATTTCGTATCAACTTT
TGTATCCACAGTAGACAAAATAGAAGGAATCCACATGCCTATTGCTGGGTGTTGAATGACAGACAATCTTATGTAGCA
GAGATTATGCCTGGGAAGGAAAATTATTCAGGGCAGCTAATTTTGCTTTTACCAAAATATCTGTAGTAATATTTTTGG
ACAGTAGCTAATGGGTCAGTGGGTTCTTTTTAATGTTTATACTGAGATTTTTCTTTTACAAAAATAAAAACAAAAATTA
AAAAAAAAAACCTTCTAGGACTTTAGATGATGTAATACCAGCTAAATCCAAACAATACTCTAGTGGAGGGTTTTACAT
TATCCCATCTACTGTGTTTGTATTCATGCTATGATAATAAGTTTGAAATGGGCAAAGAACATCAGACAGCTGAAGTGTT
AGCCCACAAGTTTCAAACAATGTTTGGAAATCTCTTTTTACCCTTAACTGAAGTGCCAATTTTGAGCAGCTGACATCT
TTCAGCTGCTATCGTGTTGGAGCATTGGGGACATGCTAGAGAGGCTTAATTGTACTTTACCCTCACCTGGAGGTAATT
TAAAATTTGAATGTCACAATCTACTCAAAGAGTCAGCATGAGGTGGGTAGGGAGATATGGGAATTTGAATAACAGGT
GGGGAAATAGGAATAGAGAGTTTAGGAATTATCCTGGCATCCTGAGTACGCCCCAGGTTTCAGAAGTTCACTTCTGT
CTGCACTGTAATAAAGTAATACTAGCTCTACTGGCAGCCATTTCCAAAATGGCAATTTGAGTTCCAAGGAAGAGAGT
AGCGGCAACAGTGAAATCCAAAGAAAAATCTAGCATGGGGTCTGCCTAAGTTTCTTTTAGCCATTGCTTACCTTGCC
AATTTGATTCTGGTCATCCAAAGAAAAGATGCTATCAATGTAGGTGACAATGTCTAGACCCCAAGGAAGTTGTGTCTT
TGACAGATTTCCCTGGTAACATTGGAGATATGACTTTCCATGCCATATCTTATGCCTTTGGGGCTGAACAAATAAGCG
ACTTACTGATAATTTCTTTTTAATCACATGTCGTGTTCATACTTTGAAGTCATACATTGAAAGGTCATTGTCCAGCCATT
GGTTTGGAGTTACCCATACACCTGCATGAAGTTGATTACAAGTCTCTTTCTACTCATACTTTGCAACTCTGAGATTTAC
TGTGGATACTGAGAATGATCACTAGGACCATAGTAATGTCTAATATTCACAGTCAGACCTGCTTAGGGAACCTAAGTC
TTTTAAAGGCAAATAGAGTCATACAGTAGCACATAAGGCAACCATGACTCTCTTTGGTACAGGTCTTTGGAGGTTGA

TCCAGCTTACACTGCACACATCCTAGATTAACTCCATGAAAATTTACTCTCTTGCAAATGGAGCAAACACATTTAACTG
TGGTCCCAAATATCCATCTTTTCATTAGTGTGAATATGCTCTATTTCTAGCTTCATAGCCTATCCATTTAAATTAAAGTGT
GGTCTCTTTTAAAGTCCTTTAGACTTGCTTTCTAAGTGATTATGTCTCAATTTTTGCACTGTGCTTCGGAGACTTAAGA
GAAATTTCCCCTTTCTTTTACATCCGAATGTGCCTGAACTTTTTCAAATATGTAAATGCTACCATGTTCCAAACCCATCT
TTAGTGTCTTTGTATGGAGCTGTGCACCCTGGAAATAACACAGAGTCCCAGGAGCAGGTGCCTGAGACATGGACCC
CTTTGTAGTCACAGAGAGGTCATTGGTCGTCGAGACTTGAATTAATAAGTGACATCACGCCAGTTTATTTTCCTTCAC
AGCGTACAAACAACGCTTTCTGTGCACTACATATTCTTCAGTGTAGAGTTCTTGTTTTTCGGGGAGAGGCACAGATG
CCCCATTGTGTTGGATGGATTACTACAGGCTTCTGATGCACACTGCTATTGATGTGACCCCGTTTCATCGCCGCTTTGC
TTTGTTTAATGAAACACACGTGTATGCCTCTTTTGCACCTTGAAATGGTAAAGAATCCAGTGGGATGCTCAAGCCCCT
GTAAACCATCTTCTCAGCATATTCAATGTTCAAATAAAAAATAAAATAAAGGCA

***(a) Esr1* 3'UTR fragment cloned for reporter assay**

Fragments	**Start**	**End**
Esr1	3484	4190

(b) miRNA binding sites

miRNA site	**Position**	**WT sequence**	**Mutated sequence**
miR-130b	3644-3650	TTGCACT	TAGGAGT
miR-130b	3926-3932	TGCACTA	TCCTCAA

***2. Pten* 3'UTR**

TTTTTTTTTTCTTATCAAGAGGGATAAAATACCATGAAAAAAAAAAAACTTGAATAAACTGAAATGGACCTTTTTTTT
TTTTTTTTTTTTTTAAATGGCAATAGGACATTGTGTCAGATTGCAGTTATAGGAACAATTCTCTTCTCCTGACCAATCTT
GTTTTACCCTATACATCCACAGGGTTTTGACACTTGTTGTCCAGTTAAAAAAAGGTTGTGTAGCTGTGTCATGTATATA
CCTTTTTGTGTCAAAAGGACATTTAAAATTCAATTAGGATAAATAAAAGATGGCACTTTCCCATTTTATTCCAGTTTTA
TAAAAAGTGGAGACAGGCTGATGTGTATACGCAGGAGTTTTTCCTTTATTTTCTGTCACCAGCTGAAGTGGCTGAAG
AGCTCTGATTCCCGGGTTCACGTCCTACCCCTTTGCACTTGTGGCAACAGATAAGTTTGCAGTTGGCTAAGGAAGTT
TCTGCAGGGTTTTGTTAGATTCTAATGCATGCACTTGGGTTGGGAATGGAGGGAATGCTCAGAAAGGAATGTTTCTA
CCTGGGCTCTGGACCATACACCATCTCCAGCTCCTTAGATGCACCTTTCTTTAGCATGCTCCACTTACTAATCTGGACA
TCCGAGAGATTGGCTGCTGTCCTGCTGTTTGTTTGTGCATTTTAAAGAGCATATTGGTGCTAGACAAGGCAGCTAGA
GTGAGTATATTTGTAGTGGGGTACAGGAATGAACCATCTACAGCATCTTAAGAATCCACAAAGGAAGGGATATAAAA
AAAGTGGTCATAGATAGATAAAAGACACAGCAGCAATGACTTAACCATACAAATGTGGAGGCTTTCAACAAAGGAT
GGGCTGGAAACAGAAAATTTGACAATGATTTATTCAGTATGCTTTCTCAGTTGTAATGACTGCTCCATCTCCTATGTAA
TCAAGGCCAGTGCTAAGAGTCAGATGCTATTAGTCCCTACATCAGTCAACACCTTACCTTTATTTTTATTAATTTTCAAT
CATATACCTACTGTGGATGCTTCATGTGCTGGCTGCCAGTTTGTTTTTCTCCTTAAATATTTTATAATTCTTCACAGGAA
ATTTCAACTTGAGATTCAACAGTAAGCAGGTTTTGTTTTTTTTTTTTCCTAGAGATTGATGATGCGCGTCCTCAGTCC
AGTGGCTGTCAGACGTTCAGCCCCTTTGACCTTACACATTCTATTACAATGAGTTTTGCAGTTTTGCACATTTTTTTTA
AATGTCATTAACTGTTAGGGAATTTTACTTGAATACTGAATACATATAATGTGTATATTAAAAAAGTCATTGTTTGTGTT
AAAAAAGAAATTAGAGTTGCAGTAAATTTACAGCACTGCACGAATAATAAGGCATTGAAGTTTTTCAGTAGAAATTG
TCCTACAGATGCTTTATCGACTTGCTATTGGAAGAATAGATCTTCTTAAATGTGCAGTGTTGAGTCACTTCGTTATAGT
GGTAGAGTTGGGATTAGGGCTTCAATTTTACTTCTTAAATATCATTCTATGTTTGATATGCCCAGACTGCATACAATTTA
AAGCAAGAGTACAACTACTATCGTAATGGTAATGTGAAGATGCTATTACAAAGGATCTCCTCCCAACCCCTCGGGAAT
TTGGTGTCTTTCAAATTATATCTTGACCTTGACATTTGAATATCCAGCCATTATTAGATTTCTTAATGGTGTGAAGTCCC
ATTTTCAATAACTTATTGGTGCTGAAATTGTTCACTAGCTGTGGTCTGACCTAGTTAATTTACAAGTACAGATTGCATA
GGACCCACTAGAGAAGCATTTATAGTTTGATGGTAAGTAGATTAGGCAGAACGCCATCTAAAATATTCTTAGAAAATA

ATGTTGATGTATTTTCCATACCTCATCAGTTTCACTCAACCAATAAAGTTTTTAAAATTGTAACAAAGCTCTTAGGATTT
ACACATTTATATTTAAACATTGATACATGAATATTGACTGACTGTTGATAAAGTCAGAGACAACTTTTCCTGAGATCTC
ACCATGGAAATCTGTACACCCCCTTGTCTTTCCTAAAAGCTGAAAGTGGCTGACTAAAATGCAAAGCAGCTGTTGAT
GTTTTGAAGATAGTGATAAACACTGTTCTTTGTTAGTTTTGGGCACAGCATGCTAAACTATAACTTGTATTGTTCCAAT
ATGTAACACAGAGGGCCAGGTCATGAATAATGACATTACAATGGGCTGTTGCACTGTTAATATTTTTCCTTTGGAATG
TGAAGGTCTGAATGAGGGTTTTGATTTTGAATGTTTCAGTGTTTTTGAGAAGCCTTGCTTACATTTTATGGTGTAGTC
ATTGGAAATGGAAAAATGGCATTATATATATATTATATATATATAAATATATATATTATACATACTCTCCTTACTTTATTTCAG
TTACCATCCCCATAGAATTTGACAAGAATTGCTATGACTGAAAGGGTTTTGAGTCCTAATTCAAACTTTCTTTATGACA
GTATTCACGATTAGCCTGAAGTGCATTCTGTAGGTGATCTCTCCCGTGTTTCTGGAATGCTTTCTTAGACTCTTGGATG
TGCAGCAGCTTATGTGTCTGAAATGACTTGAAGGCATCACCTTTAAGAAGGCTTACAGTTGGGCCCCGTACATCCCA
AGTCCTCTGTAATTCCTCTTGGACATTTTTGCCATAATTGTAAAAGGGTAGTTGAATTAAATAGCGTCACCATTCTTTG
CTGTGGCACAGGTTATAAACTTAAGTGGAGTTTACCGGCAGCATCAAATGTTTCAGCTTTAAAAATAAAAGTAGGTT
ACAAGTTACATGTTTAGTTTTAGAAAATTTGTGCAATATGTTCATAACGATGGCTGTGGTTGCCACAAAGTGCCTCGT
TTACCTTTAAATACTGTTAATGTGTCGTGCATGCAGACGGAAGGGGTGGATCTGTGCACTAAACGGGGGGCTTTTAC
TCTAGTATTCGGCAGAGTTGCCTTCTACCTGCCAGCTCAAAAGTTCGATCTGTTTTCATATAGAATATATATACTAAAAC
CATCCAGTCTGTAAAACAGCCTTACCCCGATTCAGCCTCTTCAGATACTCTTGTGCTGTGCAGCAGTGGCTCTGTGTG
TAAATGCTATGCACTGAGGATACACAAATATGACGTGTACAGGATAATGCCTCATACCAATCAGATGTCCATTTGTTAC
TGTGTTTGTTAACAACCCTTTATCTCTTAGTGTTATAAACTCCACTTAAAACTGATTAAAGTCTCATTCTTGTCATTGTG
TGGGTGTTTTATTAAATGAGAGTATTTATAATTCAAATTGCTTAAATCCATTAAAATGTTCAGTAATGGGCAGCCACATA
TGATTACAAAGTTCCTGTGCATTTTTCTATTTTTCCCCCTCCTTGCTATCCTTCCAAGCAAAGCATCTTTCTGTCATCTT
GGTAGACACATACCTGTCTACTCATGGTTAAGAAGAGCACTTTAAGCCTTAGTCATCACTTAATAAGTTATTCCAGGC
ACAGTAAAAAGTTCAAGGTTCTTGGAAAACGGTGCTTATTTCTCTTCTTATAAGCCAGATGTCTGAAGATAGCCCTAA
CCCCAAGAACGGGCTTGATGTCTCAGGTCTGTTCTGTGGCTTTCTGTTTTTTTTAACACTGCAGTTGGCCATCAGCAC
ATGGGAGGTTTCATCGGGACTTGTCCAGAGTAGTAGGCTCAAATATACTATCTCCTTTCTAATATTCTTAAAGGCTAAG
GAGTCCTTTCAATATAACAGTAAGATAACTTGTGATGTTTTAGAAGTAAGCAGACCATTAATGTCAATGTGGAGTCTT
AATGTTACATGAAGTTGATAGTTTCTCTGTGACCCATTTAAAAATACAAACCGAGTAGCATGCAATTATGTAAAGAAAT
ATGAAGATTATATGTAGTCACACATTTTCTTTAGAATTCTTAGTTTGGTGAAAACTTGAATATAAAGGTATTTTGATTTA
TATGACATTTTGATGATATTTGAAAAAAAGGAATTTCCTGACATTTTGCTTTTAGATCATGTCCCCCATTGTGCTGTAAT
TTAAGCCAACTTGGTTCAGTGAATGCCATCACCATTTCCATTGAGAATTTAAAACTCACCAGTGTTTAACATGCAGGC
TTCTGAGGGCTCCCGGAGAATCAGACCTTAAGCCCAGTTGATTTACTTCTAACGTGAAACTTCGAGTTCCTGTATACT
TTGCTAGATAATTTGTGGTACATCTAAAGCTTAGTCTTAAGTGGCTTGTGTGTGGATTTTATTCAACATTCTTGTTGCTA
GGGTAGAGAGAAATGTTGCTGAGTAGAAACAAGAGTACCCAGTTCAATGTGGTACAGAGAGCAGTCCCTAAAATCT
GTACACAGTGTAATGGACCACTTTAGGAGTCAAGAGGCTGATTTTTCCTATGAAATTACATTGCAACAGGAAGCCTT
CTAGTATAGTTCCTTTTACTGTTAGAATATGTTTTTATGCATACGCTATAGCTGCTTTCCCATCTTCCAACAACAGGTATC
AGGATGTAAGCAAGCTTTAAACAGTGTGAAGATGGCAGGATAGTGTCATCGGTAACAGTCCTCTGACTCTAAATGTA
GTTGCTCTGTAACACTTTGTGAATATAACATCACAATTCTCATGTCCTTGGGGGGGGGGGCATACCCAGTATTAGTA
TGTTTTAGTGACTAAGCAATCATTTTTCTGTTTACTCATGTACATTTTCTCTTTAAAACTAAAACCTGTACTGTGTATGTC
TCCAAAGCCTTTTAGCTTAGTTTTTAGGAAATGAACACTGAATGGATCACTTTTTAGTGTAGCAGGTATGGGATATGT
GCATTATAGAGAGACCTTGTCAGCTCTCTGGGCCTATTTGAATGTTTATTGTTGGTGTGAGGATGGTAGGGGAATCA
GTAAATACAAGTTACGTTGGTTTAGCAGAGCAAGCTCAGTGTGGGTATTTCTCTTTGAAGCGTGGTGCGTGACGCAC
TGTGAGTAGAGAATTTGGTCACCCTTTGAGTCCTCTTGCATTTTGCAAACTTGCTCAGCAAATGCGTACCTACCTTGC
CCCCTAGGTAAAAGCAGGAACTACTACTGATTTATCTGTCACTCAGCTGTCTTTATATGTGTGCTTCTGTGACTTGTATC
ACACAAGAATCTTAAAGATTTCACAAATTGTTACCTTTTAGCTCTGAATGTTGAGTATTCTGGTGGGCTAACAACAAG
ACAAACTCTTGACAGTCATTTGAGAATTTTCATGAAACATTTAGCTGAAAACATTTTATAATTTATGAAAAAAATGTGT
TACCTTAAACTTTTACATATGTGGGAGACATTAACTGCCATATTTGAGCATACTGAATTTTAAATTTAAAATAAAGCTGC
ATATTTTTAAATGAAATGTTTAACAAGGATTCATATTTTTTGTTTTTTAAGATTAAAAATAATTTATGTCTTCTCATGTGG
AACCTCATCTGTCACAATGGTTAGATTATACAGAATGGAGCAAGGCTTGTAGTGGTTTAGCTTACAGTAAAATTCTTA
ATGTTTAGATGTGTTTACTTACTGGCTGTTATGTATACTTTTGAGATTTTCCACCTGTTCTGTGTAGTTTTCTAAATGATA
CTCCTACTTAAAAACAGCATTTTAGTATCTATTTTCTGTCTCCATTAAATGGTCCTCATTTTCTATTGAGTTTGGAAGTG

TGCACATTGTGTGTGTGTGTGTGTGTGTGTGTGTGCACACGTGTGCGCGCCCGTGCGTGTGTCTATTTGTGGAGTTT
GTATGGGAGAATTAGTTTTGAAAGTGCTAGAATAGAGATGAAATTTGGTTCAAGTAAAATTTTCCCACTGGGATTTTA
CAGTTTATTGTAATAAAATGTTAATTTTGGATGACCTTGAATATTAATGAATTTGTTAGCCTCTTGATGTGTGCATTAAT
GAGATATATCAAAGTTGTATATTAAACCAAAGTTGGAGTTGTGGAAGTGTTTTTATGAAGTTCCGTTTGGCTACCAAT
GGACATAAGACTAGAAATACCTTCCTGTGGAGAATATTTTTCCTTTAAACAATTAAAAAGGTTCATTATTTTTGA

***(a) Pten* 3'UTR fragment cloned for reporter assay**

Fragments	**Start**	**End**
Pten	1902	3432

(b) miRNA binding sites

miRNA site	**Position**	**WT sequence**	**Mutated sequence**
miR-130b	2247-2253	TTGCACT	TAGGAGT
miR-130b	2962-2968	TGCACTA	TCCTCAA

Extended Data Table 4| Demographic and clinical data of the patients with multiple sclerosis included in the study.

	MS patients (n=41)
Demographics	
Women. n (%)	22 (53.7%)
Age (years)	43.12 (9.43)
Clinical data	
Time from diagnosis (months)	96.03 (108.86)
Baseline SDMT	47.40 (13.53)
Brain volume (cc)	1119,85 (156,86)
Gray matter volume (cc)	603,45 (72,07)
Cortical gray matter volume (cc)	710,21 (1206,50)
Caudate nucleus volume (cc)	6,68 (1,12)
Cerebellum volume (cc)	7137,24 (15,97)

* All values represent mean (SD) unless otherwise indicated.

Abbreviations: CC, cubic centimeters; N, number; SD, standard deviation; SDMT, symbol digit modality test.

Materials and Methods

Mice

The generation of IgM^{b}-macroself mice (MMRRC Strain 36510), *Pten*$^{fl/fl}$ mice (Jax stock 006440), and *Esr1* knockout mice (Jax stock 026176) was previously described (*11, 33-35*). Mice were housed and bred in the animal facility of Institute for Biomedical Research, Autonoma University of Madrid under specific pathogen-free conditions. All animal experiments were approved by Animal Care and Bioethics Committee of Institute for Biomedical Research, Autonoma University of Madrid, and Community of Madrid, Spain.

Retrovirus production

Retroviruses were generated by cotransfecting HEK293T cells with constructs encoding miR-130b, miR-33, miR-210 or an empty vector (control) from the pMIRWAY library, which includes green fluorescent protein (GFP) as a reporter, alongside GAG-POL and VSV-G plasmids. Confluent HEK293T cells were plated at a dilution 1:5 the day before transfection. Cells were co-transfected with individual miRNAs or control plasmids, and packaging constructs. Cell culture medium was replaced after 24 hours. At 48 hours post-transfection, virus-containing supernatants were harvested, filtered, aliquoted, and stored at -80°C until use. Viral titers were determined by serial dilution (1:5) of the viral supernatants and analysis of GFP expression in infected target cells 48 hours after infection.

Cell lines

WEHI-231 cells and their derivatives were grown in DMEM with 10% FBS, 2 mmol/l L-glutamine and Pen/Strep, and 50 µM 2-mercaptoethanol. The stable cell lines WEHI-control and WEHI–miR-130b were generated by retroviral transduction of WEHI-231 cells with particles encoding miR-130b or an empty construct (control), and enrichment with FACS. Specifically, WEHI-231 cells at $0.5x10^{6}$ cells/ml were transduced with MSCV-control-GFP or MSCV-miR-130b-GFP retroviral particles in the presence of 8 µg/ml polybrene. Cells were expanded for 48 hours, sorted by FACS to enrich the GFP^{+} infected population, grown for an additional 48 hours, aliquoted and stored in liquid nitrogen until use.

Bone marrow transduction and reconstitution experiments

Donor 6-8 weeks-old C57BL/6J mice were injected with 5-fluorouracil (Sigma) at a concentration of 150 mg/kg. After 4 days, bone marrow cells were isolated and HSPCs were enriched by Ficoll (GE Healthcare) density-gradient centrifugation. Cells were resuspended in X-vivo 15 medium (Lonza) supplemented with 10% BSA, 2 mmol/l L-glutamine and Pen/Strep, 100 µM 2-mercaptoethanol, 100 ng/ml mSCF, 50 ng/ml mTPO, 50 ng/ml mFlt3L and 20 ng/ml mIL-3, and transduced overnight with retroviral particles on retronectin-coated plates (Takara) in the presence of 2 µg/ml polybrene (Sigma Merk). Following infection, cells were retrieved, washed with excess PBS, and injected into the tail vein of recipient 8-12 weeks-old IgM^{b}-macroself mice that had been previously

irradiated (on the same day) with two doses of 5.0 Gy separated by 3 hours. Both female and male recipient mice were used. Each recipient mouse received 2×10^6 to 5×10^6 infected cells mixed with 0.5×10^6 helper bone marrow cells from CD45.1$^+$ C57BL/6J mice. 8 weeks after reconstitution, recipient mice were euthanized and the presence of B cells in the spleen was determined by cell surface staining with anti-CD19-PE (6D5; BioLegend) and anti-IgM-Cy5 (115-175-075; Jackson ImmunoResearch), and flow cytometry analysis in a FACS Canto II (Beckman Dickinson). Data were analyzed using the FlowJo, LLC V10 software.

Purification of murine primary immature B cells

Femur and tibia bones were isolated from C57BL/6J mice, and their bone marrow cells retrieved by flushing in PBS 2% FBS. Cells were washed twice with PBS 2% FBS and enriched for B cells using magnetic beads (Miltenyi Biotec). Cells were then stained with anti-IgM-Cy5 (115-175-075; Jackson ImmunoResearch), CD19-BV421 (1D3; BD Biosciences) and CD93-PeCy7 (AA4.1; eBioscience). Immature B cells, defined as CD19$^+$-IgM$^+$-CD93$^+$ cells, were sorted in a Moflow ASTRIOS Sorter (Beckman Coulter). Purified immature B cells were washed once with PBS and stored at -80 °C until use.

Quantitative RT-PCR

WEHI-control and WEHI–miR-130b cells were stimulated with 2 µg/ml anti-IgM (115-175-075; Jackson ImmunoResearch) for 14 hours and total RNA was extracted from the cells using TRI Reagent (Invitrogen), following the manufacturer's instructions. Total RNA from purified mouse immature B cells was prepared using the RNeasy Micro Kit (Qiagen). cDNA was synthesized by reverse transcription of total RNA (1 µg) with the High-capacity cDNA reverse transcription kit (Applied Biosystems). Quantitative RT-PCR was performed using the Power SYBR Green PCR Master Mix System (Applied Biosystems) with specific primers for mouse *Cfl2, Esr1, Prkaa1, Pten, Runx2* and *Sos2*, using *Actb* for normalization. The following primers were used for quantitative RT-PCR analysis: *Cfl2* 5′-GCATCTGGAGTTACAGTGAATGA-3′ and 5′-CACCAATGTCACCCACCAAGA-3′; *Esr1* 5′-CCCGCCTTCTACAGGTCTAAT-3′ and 5′- CTTTCTCGTTACTGCTGGACAG-3′; *Igf1* 5′-CTGGACCAGAGACCCTTTGC-3′ and 5′-GGACGGGGACTTCTGAGTCTT-3′; *Prkaa1* 5′-GTCAAAGCCGACCCAATGATA-3′ and 5′-CGTACACGCAAATAATAGGG GTT-3′; *Pten* 5′-TGGGGAAGTAAGGACCAGAG-3′ and 5′- GGCAGACCACAAACTGA GGA-3′; *Runx2* 5′-AAAGCCAGAGTGGACCCTTCCA-3′ and 5′-ATAGCGTGCTGCCATT CGAGGT-3′; *Sos2* 5′-CAAGATGTTGAGGAACGAGTTCA-3′ and 5′-TGTCCACAGGTA GTAAGAGAGGA-3′; and *Actb* 5′-CTAAGGCCAACCGTGAAAG-3′ and 5′-ACCAG AGGCATACAGGGACA-3′.

Western blot

Dry cell pellets were resuspended in RIPA lysis buffer (150 mM NaCl, 1% NP-40, 0.5% Sodium deoxycholate, 0.1% SDS, 25 mM Tris pH 7.4, and ddH_2O) supplemented with protease inhibitors (Roche) and phosphatase inhibitors (Sigma-Aldrich). Protein quantification was performed using the BCA assay (ThermoScientific). Protein extracts

(10 μg per sample) were resolved on 10% SDS-PAGE gels and transferred onto nitrocellulose membranes (GE Healthcare). Membranes were blocked in TBS-0.1% Tween-20 (TBS-T) containing 5% BSA for one hour at room temperature, followed by washing with TBS-T. The membranes were then incubated overnight at 4°C with primary antibodies specific for ERα (Santa Cruz Biotechnology, sc-542), PTEN (Cell Signaling, 138G6), and β-actin (Santa Cruz Biotechnology, sc-47778). After extensive washing with TBS-T, membranes were incubated for one hour at room temperature with goat anti-rabbit or goat anti-mouse horseradish peroxidase-conjugated secondary antibodies (Santa Cruz Biotechnology). Bound antibodies were detected using the Clarity Western ECL Substrate (Bio-Rad) and visualized using a Fusion Solo S (Vilber) chemiluminescence imaging system.

Dual luciferase reporter assays

The sequence encoding miR-130b was cloned into the expression vector pCXN2, and 3′ UTR fragments of *Esr1* and *Pten* were cloned into the psiCHECK2 vector (Promega). The miR-130b binding sites in the 3′ UTR of each target gene were mutated with the QuikChange Multi Site-Directed Mutagenesis Kit (Agilent Technologies). The resulting pCXN2 and psiCHECK2 plasmids were transfected into HEK293 cells using Fugene HD (Promega) according to the manufacturer's instructions. After 24 hours, cells were lysed, and luciferase expression was measured using the Dual-luciferase assay system (Promega) following the manufacturer's protocol. The renilla luciferase activity was normalized to that of firefly luciferase, and the ratio of renilla luciferase activity to firefly luciferase activity was arbitrarily set as 1 for the control pCXN2 vector for each psiCHECK2 reporter.

Bone marrow transplantation

Donor bone marrow was harvested from 6-8 weeks-old mice of indicated genotypes and used to reconstitute lethally irradiated 8-12 weeks-old IgM^b-macroself mice. For each recipient mouse, 2×10^6 to 5×10^6 donor bone marrow cells were mixed with 0.25×10^6 helper bone marrow cells from $CD45.1^+$ C57BL/6J mice and were inoculated intravenously into IgM^b-macroself mice that had been previously irradiated (on the same day) with two doses of 5 Gy separated by 3 hours. Both female and male recipient mice were used unless otherwise stated. Splenocytes were analyzed 8 weeks after reconstitution to determine the presence of B cells by staining with anti-CD19-PE (6D5; BioLegend) and anti-IgM-Cy5 (115-175-075; Jackson ImmunoResearch) and flow cytometry analysis as above.

Determination of miR-130b levels in EVs of patients with multiple sclerosis

An observational, longitudinal, and prospective study was conducted, including patients with a confirmed diagnosis of relapsing-remitting multiple sclerosis (RRMS), based on the McDonald criteria, from May 2021 to June 2023. Only patients not receiving immunomodulatory treatment were included. The study was approved by the Research Ethics Committee of La Paz University Hospital (PI-4675), and informed consent was

obtained from each participant. Demographic and clinical data collected included sex, age, disease duration, Symbol Digit Modalities Test (SDMT) scores, new white matter lesions on T2-weighted MRI sequences, total brain volume, and the volumes of specific structures, including white matter, gray matter, cerebellum, hypothalamus, and basal ganglia, assessed using 3D T1 and FLAIR sequences and analyzed with aCloud and Freesurfer v5.3.0.

Blood samples were collected in 9 mL EDTA tubes and centrifuged at 1800 rpm for 15 minutes to isolate cell-free plasma. For extracellular vesicle (EV) isolation, 1 mL of plasma per patient was thawed rapidly in a 37°C water bath, transferred to a 1.5 mL Eppendorf tube and centrifuged at room temperature for 20 minutes at 2000g. EVs were isolated using the ExoQuick EV isolation kit (System Biosciences, USA). miR-130b content in EVs was analyzed using miRNA sequencing. Total RNA was extracted from EVs with the miRNeasy Serum/Plasma Advanced Kit (Qiagen, USA). Library preparation was performed from 10 ng of total RNA per sample with the SMARTer smRNA-Seq Kit (Illumina, USA) and validated for size, purity, and concentration using the Agilent Bioanalyzer (Agilent Technologies, USA). Samples were pooled in equimolar amounts and sequenced on the Illumina HiSeq 2500 platform to generate 101 base pair reads. Read quality was assessed with FastQC (Babraham Bioinformatics, UK), and sequences were trimmed and quality-filtered with Cutadapt v4.7. High-quality reads were aligned to miRNA sequences from miRBase v22 using the mirDeep2 tool.

Bioinformatic analyses

For Multiple Em for Motif Elicitation analysis, a list of 101 lymphocyte-expressed miRNA families was generated from available expression profiling data (*18*) and the nucleotides in positions 1-8 filtered as a FASTA file. This was submitted as input for analysis in Multiple Em for Motif Elicitation (MEME) suite (https://meme-suite.org/meme/tools/meme) as previously described (*17*). The output was ranked by MEME based on the E-value obtained for each motif.

To identify protein-coding genes with potential function in B cell tolerance, the predicted target genes of miR-130b, miR-19b and miR-148a were determined individually through RDB miRNA mining (*36*). The common targets were then selected, and the resulting 110 genes subjected to Ingenuity Pathway Analysis (IPA, Qiagen) for identification of potential functionally relevant signaling pathways regulated by these miRNAs.

Statistical analysis

Data were analyzed using an unpaired two-tailed Student's T test. Statistical significance was defined as * $P \leq 0.05$, ** $P \leq 0.01$, *** $P \leq 0.001$ and **** $P \leq 0.0001$. Bar graphs show mean + s.e.m or mean + s.d., as indicated for each Figure.

Data availability

All data included in this manuscript are available from the corresponding author, A.G-M., upon reasonable request.

Acknowledgments

We thank Luis del Peso for his help with the MEME analysis. We also thank the personnel from the animal facilities at IIBM and UAM, and from UAM Flow Cytometry Core for technical assistance. This work was supported by the grants RTI2018-100008-A-I00 MCIN/AEI/10.13039/501100011033 and FEDER, PID2021-128244OB-I00/AEI/FEDER 10.13039/501100011033 and CNS2022-136069/MCIN/AEI/10.13039/501100011033 and European Union "NextGenerationEU"/PRTR from Spanish Ministry of Science and Innovation, SI1-PJI-2019-00241 from Community of Madrid, LABAE20001GONZ from Spanish Association Against Cancer (AECC), XXIII Beca FERO from FERO Foundation, and XXI National Research Grants in Life Sciences from Ramon Areces Foundation to A.G-M. A.G-M was supported by merit award RyC-21155 MCIN/AEI/10.13039/501100011033 and FSE and L.G-R by the PRE2019-087940 FPI fellowship from Spanish Ministry of Science and Innovation. MdP.G-M. was supported by an FPI-UAM 2020 fellowship from Autonoma University of Madrid and L.M. by the PEJ-2020-AI/BMD-17617 contract from the Garantia Juvenil Program of Community of Madrid.

Author contributions

A.G-M. conceptualized and designed the project and wrote the manuscript with contributions from all authors. B.H-F., MdP.G-M., AM.P-M., J.S-G., T.G-S., A.M., and A.G-M. performed experiments. L.G-R. performed bioinformatic analyses. MP.L-M and L.O. performed all experiments with samples of patients with autoimmunity and provided materials and reagents. L.M. managed and genotyped the mouse colonies, and provided technical support. D.N. and C.X. supported experiments and provided materials and reagents. A.G-M. obtained funding and supervised the project.

Competing interest declaration

The authors declare no competing financial interests.

Corresponding author

Correspondence to Alicia González-Martín: agonzalez@iib.uam.es

References

1. E. Zerhouni. (Progress in autoimmune diseases research. N.I.o.H. U.S. Department of Health and Human Services, ed. , 2005).
2. N. Conrad *et al.*, Incidence, prevalence, and co-occurrence of autoimmune disorders over time and by age, sex, and socioeconomic status: a population-based cohort study of 22 million individuals in the UK. *Lancet* **401**, 1878-1890 (2023).
3. F. W. Miller, The increasing prevalence of autoimmunity and autoimmune diseases: an urgent call to action for improved understanding, diagnosis, treatment, and prevention. *Curr Opin Immunol* **80**, 102266 (2023).
4. K. S. Forsyth, N. Jiwrajka, C. D. Lovell, N. E. Toothacre, M. C. Anguera, The conneXion between sex and immune responses. *Nat Rev Immunol*, (2024).
5. M. J. Shlomchik, Sites and stages of autoreactive B cell activation and regulation. *Immunity* **28**, 18-28 (2008).
6. S. Yurasov *et al.*, Defective B cell tolerance checkpoints in systemic lupus erythematosus. *J Exp Med* **201**, 703-711 (2005).
7. L. Menard, J. Samuels, Y. S. Ng, E. Meffre, Inflammation-independent defective early B cell tolerance checkpoints in rheumatoid arthritis. *Arthritis Rheum* **63**, 1237-1245 (2011).
8. T. Kinnunen *et al.*, Specific peripheral B cell tolerance defects in patients with multiple sclerosis. *J Clin Invest* **123**, 2737-2741 (2013).
9. D. Nemazee, Mechanisms of central tolerance for B cells. *Nat Rev Immunol* **17**, 281-294 (2017).
10. H. Wardemann, M. C. Nussenzweig, B-cell self-tolerance in humans. *Adv Immunol* **95**, 83-110 (2007).
11. B. H. Duong *et al.*, Negative selection by IgM superantigen defines a B cell central tolerance compartment and reveals mutations allowing escape. *J Immunol* **187**, 5596-5605 (2011).
12. A. Gonzalez-Martin *et al.*, The microRNA miR-148a functions as a critical regulator of B cell tolerance and autoimmunity. *Nat Immunol* **17**, 433-440 (2016).
13. M. Lai *et al.*, Regulation of B-cell development and tolerance by different members of the miR-17∼92 family microRNAs. *Nat Commun* **7**, 12207 (2016).
14. D. P. Bartel, MicroRNAs: target recognition and regulatory functions. *Cell* **136**, 215-233 (2009).
15. C. Xiao, K. Rajewsky, MicroRNA control in the immune system: basic principles. *Cell* **136**, 26-36 (2009).
16. K. M. Pauley, S. Cha, E. K. Chan, MicroRNA in autoimmunity and autoimmune diseases. *J Autoimmun* **32**, 189-194 (2009).
17. T. L. Bailey, C. Elkan, Fitting a mixture model by expectation maximization to discover motifs in biopolymers. *Proc Int Conf Intell Syst Mol Biol* **2**, 28-36 (1994).
18. S. Kuchen *et al.*, Regulation of microRNA expression and abundance during lymphopoiesis. *Immunity* **32**, 828-839 (2010).
19. S. D.-J. K. Balashov, L. Aung, Increased expression of miR-130b-5p in B cells and its modulation by glatiramer acetate in multiple sclerosis. *Journal of the Neurological Sciences* **Volume 357,** , (2015).
20. W. Wang *et al.*, Up-regulation of Serum MiR-130b-3p Level is Associated with Renal Damage in Early Lupus Nephritis. *Sci Rep* **5**, 12644 (2015).
21. A. Di Cristofano *et al.*, Impaired Fas response and autoimmunity in Pten+/- mice. *Science* **285**, 2122-2125 (1999).
22. C. D. Browne, C. J. Del Nagro, M. H. Cato, H. S. Dengler, R. C. Rickert, Suppression of phosphatidylinositol 3,4,5-trisphosphate production is a key determinant of B cell anergy. *Immunity* **31**, 749-760 (2009).
23. H. D. Phan *et al.*, CD24 and IgM Stimulation of B Cells Triggers Transfer of Functional B Cell Receptor to B Cell Recipients Via Extracellular Vesicles. *J Immunol* **207**, 3004-3015 (2021).
24. D. C. Ayre *et al.*, Dynamic regulation of CD24 expression and release of CD24-containing microvesicles in immature B cells in response to CD24 engagement. *Immunology* **146**, 217-233 (2015).

25. S. L. Klein, K. L. Flanagan, Sex differences in immune responses. *Nat Rev Immunol* **16**, 626-638 (2016).
26. M. K. Desai, R. D. Brinton, Autoimmune Disease in Women: Endocrine Transition and Risk Across the Lifespan. *Front Endocrinol (Lausanne)* **10**, 265 (2019).
27. G. J. Shim, L. L. Kis, M. Warner, J. A. Gustafsson, Autoimmune glomerulonephritis with spontaneous formation of splenic germinal centers in mice lacking the estrogen receptor alpha gene. *Proc Natl Acad Sci U S A* **101**, 1720-1724 (2004).
28. D. H. Kim *et al.*, Estrogen receptor α in T cells suppresses follicular helper T cell responses and prevents autoimmunity. *Exp Mol Med* **51**, 1-9 (2019).
29. V. Rider *et al.*, Gender Bias in Human Systemic Lupus Erythematosus: A Problem of Steroid Receptor Action? *Front Immunol* **9**, 611 (2018).
30. G. L. Mutter, M. C. Lin, J. T. Fitzgerald, J. B. Kum, C. Eng, Changes in endometrial PTEN expression throughout the human menstrual cycle. *J Clin Endocrinol Metab* **85**, 2334-2338 (2000).
31. M. M. Scully, L. K. Palacios-Helgeson, L. S. Wah, T. A. Jackson, Rapid estrogen signaling negatively regulates PTEN activity through phosphorylation in endometrial cancer cells. *Horm Cancer* **5**, 218-231 (2014).
32. K. Xu *et al.*, Extracellular vesicles as potential biomarkers and therapeutic approaches in autoimmune diseases. *J Transl Med* **18**, 432 (2020).
33. R. Lesche *et al.*, Cre/loxP-mediated inactivation of the murine Pten tumor suppressor gene. *Genesis* **32**, 148-149 (2002).
34. R. C. Rickert, J. Roes, K. Rajewsky, B lymphocyte-specific, Cre-mediated mutagenesis in mice. *Nucleic Acids Res* **25**, 1317-1318 (1997).
35. S. C. Hewitt *et al.*, Biological and biochemical consequences of global deletion of exon 3 from the ER alpha gene. *FASEB J* **24**, 4660-4667 (2010).
36. Y. Chen, X. Wang, miRDB: an online database for prediction of functional microRNA targets. *Nucleic Acids Res* **48**, D127-D131 (2020).